

Research Using RSM, Optimal Solution of Parameters for Machining Inconel 718

Faisal Shameem*

Assistant Professor, Department of Mechanical & Chemical Engineering, Galgotias University,
Greater Noida, Uttar Pradesh, India

Abstract – Inconel 718 is widely used in advanced technologies because of its special properties for engineering applications dependent on nickel. The processing of Inconel 718 is difficult and expensive because of its unique features. Current study seeks the optimization methodology of Taguchi to optimize cutting parameters with the Inconel 718 high-speed turning method. The results of the cermet tool are represented with the methodology for answer surface (RSM). The experimental strategy consists of core composite concepts (CCD). The response variables examined are surface ruggedness and flank wear. The test results showed that the proposed mathematical models could accurately characterize the performance metrics within the limits of the variables under study. The most important element affecting the surface roughness and wear of the flank is cutting pace. However, there are several considerations that make the success metrics secondary. A variance review checks the suitability of the prediction model.

Keywords – INCONEL 718, Response Surface Methodology, RSM

----- X -----

INTRODUCTION

Nowadays, it is commonly used to make parts for helicopters, racket motors, gas turbines, nuclear plants, warships, vehicles, petrochemical machinery and different high-temperature and pressure applications. Inconel-718 is an outstanding mechanical alloy. Dimensional consistency and accuracy of produced components is a must in these above-mentioned applications. Only if the right set of parameters are chosen will this be done. Due to fast job hardening during processing, Inconel-718 is difficult to cut utilizing traditional machining techniques. Act harder ensures the workpieces or tools are plastically deformed. Inconel-718 requires a considerable volume of cutting force. This results in high heat production that causes the tool's plastic deformation and thereby deteriorates its lifetime. In addition, the high chemistry of high temperatures, lower thermal conductivity and job hardening of Inconel-718 often leads to shortened workpiece material fatigue life during traditional machining. Conventional machining of Inconel718 often results in residual stresses that impede final products as in aerospace structures while surface finishing. Consequently, in contrast to modern processing technologies, machining this substance by utilizing conventional methods is very expensive.

EDM is able to create burr-free, very high L/D, aspect ratios micro frameworks. EDM is therefore fit to create different components from high-strength, durability and toughness materials. The machining of the die-sinking EDM on Inconel 718 with Cu as the tool material was explained by Bharti et al. [9]. The author determined that the release current for each measuring output is the most important input parameter. Present dumping and pulse-on-time are typical controlling criteria for surface roughness and wear intensity of the content removal rate.

In general, EDM-machined surface integrity researchers in literature are limited to the Steel instrument. Very little research was performed on EDMed surface properties for Inconel alloys to examine the interaction between wedm input parameters and the post-working surface recast sheet.

RESPONSE SURFACE METHODOLOGY (RSM)

Methodology of RSM (Reaction Surface Methodology) for machining efficiency optimization is extremely useful and new. The RSM produced in 1951 by G.E.P. Box and K.B. Wilson. The best parameter collection from the available spectrum of parameters to maximize response variables was carried out via a sequence of planned experiments. Box and Wilson introduced a polynomial for the second order to explain the importance of surface roughness and removal rates for materials. RSM is analyzed to understand the composition of the reaction surface, i.e. to understand where there is the maximum, minimum and ridge lines. RSM is a statistical method used to explore the interaction between reaction parameters and process optimization and process improvement cutting parameters. The second order polynomial model analyzes the impact on the different parameters.

LITERATURE REVIEW

Pariona et. al. and Tianchi et. al. The geometric quality properties of Al-Fe and Ni-based alloys were analyzed during laser-treated and laser beam cutting with a separate velocity. The finite element and numbered methods for laser aluminum cutting analysis and the 718-alloy layer were employees of Peirovi et al (Peirovi, Pourasghar, Nejad & Hassan, 2017) and Venkatesan et al. (Venkatesan, Kanubhai, Raval, & Vipulkumar, 2018).

Lamiki et. al. (Lamikiz et. al., 2015) Experiments were conducted with laser beam machining on 1mm thick AHSS tubes. They showed that the thickness of the laser beam and the focal position of the lens is critical for the efficiency of cutting. The laser cutting technique is best applicable to the cutting of stainless steel and mild steel specimens by Yilbas et. al. (B. S. Yilbas, Nickel & Coban, 1997) The findings of nuclear reaction research () and EDS review of the micro-particle transported x-Ray Emission () show that micro-cracks are caused by the heavy gas pressure while cutting. During the unorthodox 1-mm nitinol form alloys laser beam machining process Pfeifer et al. (Pfeifer, Herzog, Hustedt, & Barcikowski, 2010) researched efficiency parameters. Due to its outstanding properties, memory form and biological compatibility, Nitinol is one of the most challenging compounds. The impact on surface roughness and HAZ of the input parameters were also discussed.

During Nd: YAG and CO2 laser cutting of various stainless steel sheets different researchers have investigated the impact of process parameters on HAZ ("Baghjari & AkbariMousavi, 2014; Baghjari & Mousavi, 2013; S. Da Sun et al., 2018; Köse & Kaçar, 2014; Lai et al., 2017; Lawrence, Riveiro, Quintero, & Pou, 2018; Parthiban, Chandrasekaran, Muthuraman, & Sathish, 2018; Pritam, Dash, Mallik, & Parida, 2018; Sahoo & Masanta, 2015b; L. Yang, Ding, Cheng, Mohammed, & Wang, 2017; Zaied, Miraoui, Boujelbene, & Bayraktar, 2013").

Yilbas et al. (Bekir Sami Yilbas, Khan, Raza, & Keles, 2010) It was recorded that the bucket diameter differs with the strengthened content when the metal matrix compound is laser cutting. In comparison with 20% B4C reinforcement, the aluminum alloy7050 strengthened with 20% Al2O3 particles has a greater fitting diameter. Strong improvements of the top and bottom brazing with major process parameters and service time are offered in 7050 B4C-reinforced aluminum alloy. In the course of Nd: laser cutting of the 1mm thick Inconel 718 Super-Alloy layer, Ahn et al. (D. G. Ahn, Byun & Kang, 2010) experimentally explored the impact of input method parameters on qualitative characteristics. They found that the kernel width is high with

the increased cutting pace. The geometric quality test was conducted using N2 supported Nd: YAG and Co2 lasers for cutting alloy stain and Al6061 sheets, Cekic et al. (Cekic, Begic-Hadjdarevic, Kulenovic, & Omerspahic, 2014; Leone, Genna, Caggiano, Tagliaferri, & Moliterno, 2015) and Leona et al. (Leone et al., 2015). Moreover, work on Titanium and Al 7075 alloys, utilizing Nd: YAG and CO2 lasers, with respect to consistency parameters has been published (El Aoud, Boujelbene, Bayraktar, Salem, & Miskioglu, 2017, 2018; Klimpel et al., 2017; Mandal, Kuar, & Mitra, 2018).

Yan et. al. (Yan et. al., 2012). They also confirmed that laser input process parameters for the generation of 1mm thick alumina sheet striation are highly liable. The best possible input method parameters have been identified: pulse length (50-55 ns), laser capacity (360-420W), cutting speed (120-270 mm/min); pulse strength (23.7 to 34.1 mJ), focusing plane direction (0-0.5 mm) (0.5-1 mm). More has been done in the analysis of the heat impaired zone (HAZ) in laser machining of alloy material, aerospace alloy and the superalloy dependent on Inconel-718 Nickle. ("Akbari, Saedodin, Toghraie, Shoja-Razavi, & Kowsari, 2014; Anicic, Jovic, Skrijelj, & Nedic, 2017; Antar, Chantzis, Marimuthu, & Hayward, 2016; Cekic et al., 2014; Hasçalik & Ay, 2013").

Adelmann and Hellmann (Adelmann & Hellmann, 2011) Performed 1mm thick aluminum sheet fiber laser cutting process with a single parameter in the approach. The optimal range of focal location (-0.3 mm), gas pressure (12-bar) and speed (90 qm) and bowl diameter have been achieved. Optimum burr height and bowl width have been achieved (2.0 mm). For the machining of ceramic sheets several researchers have used Nd: YAG laser. They found that increased pulse energy and feed rate values have resulted in improved HAZ (Z, Lee, Ai, & L, 1996). Araujo et al. (CO2 laser used for cutting hole in aluminum alloy (Al 2024 T3) stated that shifts in microstructures were caused by HAZ (Bandi-padhyay, Sundar, Sundararajan and Joshi, 2002). In the course of the ND: YAG Inconel718 laser cutting, several researchers have also examined the results of surface, geometric and thermal parameters cutting parameters (D. G. Ahn et al., 2010; Dong-Gyu & Kyung-Won, 2009; Dubey & Yadava, 2008b). In addition, few scientists have examined the impact on the board Inconel-718 of high energy CO2 and the Nd: YAG lasers.

Reveiro et. al. (Riveiro, Quintero, Lusquiños, Comesaña, & Pou, 2010) During the 2024-T3 sheet cutting, they contrasted various modes of CO2 laser. Tests were conducted based on the complete configuration of the experiments. Better cut efficiency is obtained by high-speed cutting in the continuous mode of service. The laser cutting of fiber composite reinforced plastics was carried out by mathew et al. (Mathew, Goswami, Ramakrishnan, & Naik, 1999). RSM methodology has been used to study the parametric impact on the kerf width of cutting parameters. They found that the most important parameter was gas pressure. During the Nd: YAG method parameter laser cutting of three distinct 3 mm thick forms of polymers: polymethacrylate, polycarbonate and Polypropylene, Chaudhary and Shirley (Choudhury & Shirley, 2010) examined the effects of process parameters. Core composite design experiments were conducted. The results of gas pressure, reduction speed and laser intensity in the affected heat zone were analyzed in their work. In comparison with polycarbonate and polypropylene, they observed that the heat impacted area was less polymethacrylate.

EXPERIMENTAL DETAILS

Cutting insert

TNMG 160408 is used for the rotating test for the machinability of Inconel 718, which is made out of titanium carbide-based cermet insert. The inserts are fixed rigidly to a tool holder 2020K16 MTJNL.

Experimental techniques

A portable surface roughness tester (Taylor Hobson, Surtronic 3+) is used to calculate the surface roughness of the turned region. It has been measured and recorded at three separate sites. A new leading edge is used for each experimental test. The tests are conducted randomly. The optical reading system tool maker's microscope is used to track tool wear.

RESULTS AND DISCUSSION

ANOVA analysis

Tests are typically used in a Table of Variance Analysis (ANOVA). The ANOVA is used for the testing of the models being produced. The ANOVA aims to examine what parameters influence the response characteristics in a significant manner. The meaning test of the regression model and the importance test was conducted on each model coefficient. The ANOVA table for surface quadratic reaction model demonstrates in Table 1.

**Table 1: ANOVA table for response surface quadratic model (partial sum of squares)
(response: surface roughness, Ra)**

<i>Source</i>	<i>Sum of squares</i>	<i>df</i>	<i>Mean square</i>	<i>F value</i>	<i>p-value prob > F</i>	
Model	4.49	9	0.50	138.00	< 0.0001	Significant
A – cutting speed	3.71	1	3.71	1,026.55	< 0.0001	
B – feed	0.032	1	0.032	8.95	0.0135	
C – depth of cut	0.012	1	0.012	3.42	0.0941	
AB	0.044	1	0.044	12.04	0.0060	
AC	3.613E-003	1	3.613E-003	1.00	0.3409	Not significant
BC	4.512E-003	1	4.512E-003	1.25	0.2899	Not significant
A2	0.63	1	0.63	173.11	< 0.0001	
B2	0.095	1	0.095	26.20	0.0005	
C2	0.026	1	0.026	7.09	0.0238	
Lack of fit	0.023	5	4.600E-003	1.75	0.2768	Not significant
Pure error	0.013	5	2.627E-003			
Cor total	4.52	19				
R-squared = 0.9920			Adj R-squared = 0.9848			
Pred R-squared = 0.9541			Adeq precision = 41.241			

Results of ANOVA show that the velocity is the overriding factor that affects the Ra surface finish. Feed and cut depth contributions are 8.95 and 3.42. There are no meaningful relationships A to B and A to C and B to C. They contribute 12.04, 1.00 and 1.25 respectively. The mathematical model has been constructed using a multiple regression approach to consider the turning mechanism for surface roughness Ra. Equation gives the Ra model (2). Its R² correlation coefficient is 99.20%.

Final equation in terms of actual factors:

$$\begin{aligned}\text{Surface roughness} = & +5.719 + (0.027 \times \text{cutting speed}) - (0.053 \times \text{feed}) \\ & - (11.875 \times \text{depth of cut}) - (0.029 \times \text{cutting speed} \times \text{feed}) \\ & - (8.50\text{E-}003 \times \text{cutting speed} \times \text{depth of cut}) \\ & - (9.50 \times \text{feed} \times \text{depth of cut}) \\ & + (8.3334\text{E-}005 \times \text{cutting speed} \times \text{cutting speed}) \\ & + (32.419 \times \text{feed} \times \text{feed}) \\ & + (16.855 \times \text{depth of cut} \times \text{depth of cut})\end{aligned}$$

Table 2 summarizes the study of variation in reaction, flank wear, and shows the significant linear model. The velocity of the flank is the overriding component. Cut depth is not substantial. Its correlation coefficient is 87.42%. Other steps r^2 , modified R^2 and sufficient detail may be shown in the same table. All metrics of adequacy are similar to 1, which is rational and provides an appropriate model.

Table 2: ANOVA table for the linear solution surface model (partial sum of squares) (response: flank wear, VB)

Source	Sum of squares	df	Mean square	F value	p-value prob > F	
Model	0.041	3	0.014	37.05	< 0.0001	Significant
A- cutting speed	0.039	1	0.039	104.96	< 0.00	
B – feed	1.715E-003	1	1.715E-003	4.64	0.0468	
C – depth of cut	5.676E-004	1	5.676E-004	1.54	0.2330	
Residual	5.912E-003	16	3.695E-004			
Lack of fit	4.378E-003	11	3.980E-004	1.30	0.4097	Not significant
Pure error	1.533E-003	5	3.067E-004			
Cor total	0.047	19				
R-squared = 0.8742				Pred R-squared = 0.7965		
Adj R-squared= 0.8506				Adeq. precision = 20.851		

The sufficient accuracy ratio above 4 shows that the model discrimination is acceptable. The established mathematical quadratic models are equated in terms of actual values.

Final equation for the variables:

$$\begin{aligned}\text{Flank wear} = & -0.043 + (1.065\text{E-}003 \times \text{cutting speed}) \\ & + (0.224 \times \text{feed}) + (0.129 \times \text{depth of cut})\end{aligned}$$

The study of variance shows that the cutting pace has the most impact on the responses of the three models produced.

OPTIMISATION

Full optimization may be desired in practical manufacturing applications. A multiple response may be a cure for this. The objectives are joined together in a general desirability function, and numerical and graphical optimization can be done.

Numerical optimization

All of the input parameters chosen from Table 3 are identical (three points). The highest priority of five points shall be surface ruggedness and flank wear. Four points are provided for error

spread (POE). Table 4 shows the best two options depending on the optimization parameters selected by several numerical responses.

Table 3: Selected optimization criteria

Name	Goal	Lower limit	Upper limit	Lower weight	Upper weight	Importance (points)
Cutting speed	Is in range	100	200	1	1	3
Feed	Is in range	0.1	0.2	1	1	3
Depth of cut	Is in range	0.4	0.5	1	1	3
Surface roughness	Minimise	0.1	1.9	1	1	5
POE (surface roughness R_a)	Minimise	0.2521	6.4259	1	1	4
Flank wear	Minimise	0.08	0.285	1	1	5

Table 4: Optimal solutions using numerical multiple-responses

No.	Cutting speed	Feed	Depth of cut	Surface roughness	POE (surface roughness R_a)	Flank wear	Desirability
1	128.48	0.11	0.40	0.6649	0.2521	0.1708	0.709
2	127.39	0.11	0.40	0.6788	0.2520	0.1697	0.709

The second optimal solution in table 6 is seen in the ramps view. The program describes regions where needs satisfy the suggested parameters in a graphical optimization with many answers. The first and second optimum criteria obtained as seen in Figures 1(a) and 1(b). For surface ruggedness, the desirability rating is 0.686182 and for flank wear it is 0.556188 from the bar graph of the first optimum parameter. The desired surface ruggedness value is 0.678433 and the flank wear value is 0.562434 from the second ideal criteria bar graph.

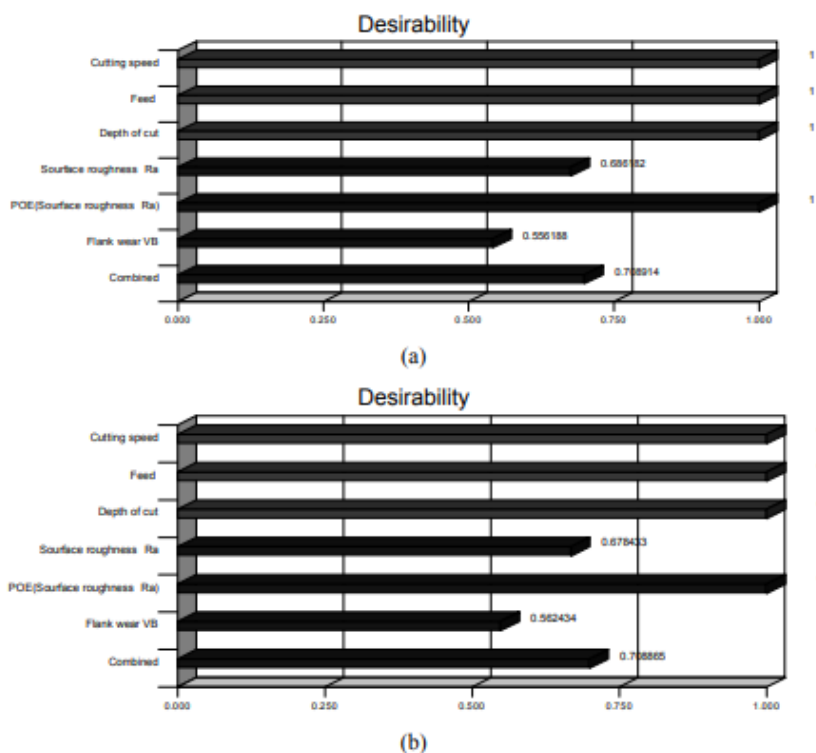


Figure 1 (a) Bar graph for the first optimal criterion (b) Bar graph for the second optimal criterion

Graphical optimization

The graphic optimization shows the field of possible factor space responsive values. The graphic improvement resulted in the overlay plot and desired plot. For a simple technical usage in a workshop, these types of plots are extremely realistic for choosing the values of the revolutions that obtain a certain answer value for this form of content. Figure 2 displays the preferability plot produced through graphical optimization for the first optimum stage. The estimated value in the figure is 0.709. The contours are rising which show that with the increasing cutting pace, the surface roughness increases.

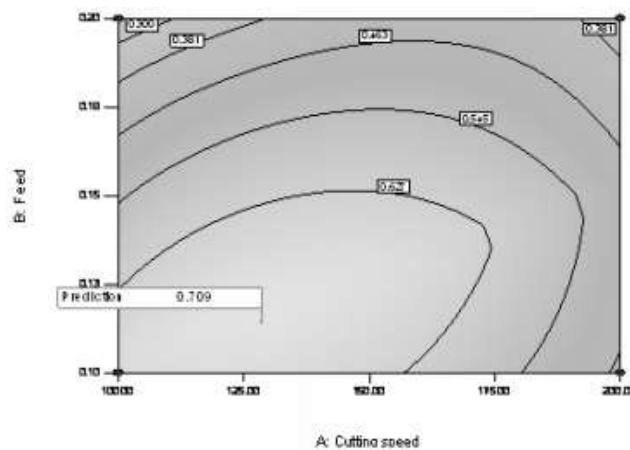


Figure 2: The desirability for first optimal point

FDS plot

In this design, a fraction of the design area (FDS) statistics are used for precision-based measurements. Figure 3 offers insights into the prediction capacity of the FDS map, yet a view of the 'rotatability' criterion of the design. The FDS graph's 'Y' axes quantify the maximum uncertainty of projection at any specified fraction of the total region. 90% of the surface architecture of this answer comes under 0.545 standard error units that can be seen in this map.

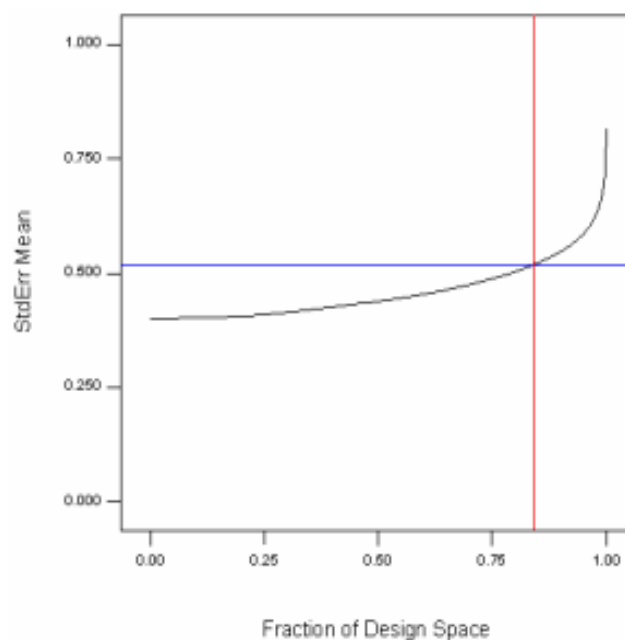


Figure 3: FDS plot (see online version for colors)

CONFIRMATION TEST

Two validation run trials are carried out to validate the suitability of the built model (Table 5). The forecast values and the resulting interval of projection are dependent on the previously existing model. The forecast model value is compared and the real experimental value determined. Table 5 shows both these values and the error in percentage is 10%. The error distribution between the real and the expected Ra and VB values is as follows: Ra -4.356 to 9.9663%, and VB -5.1807 to 10.414%.

Table 5: confirmation test

No.	Surface roughness (R_a)			Flank wear (V_B)		
	Experimental value	Model value	% error	Experimental value	Model value	% error
1	0.732	0.7100	9.032	0.193	0.1729	10.414
2	0.297	0.2674	9.966	0.266	0.2438	8.3120
3	0.294	0.2504	4.356	0.332	0.3148	5.1807

It can be said that the established empirical models, especially for Ra, are relatively precise. Both true values are below the 95% estimation interval for validation run.

CONCLUSIONS

This article describes the results from an experimental review of the effects on the roughness and flank wear of the feed rate, cutting pace and depth of cutting in Inconel 718. The ANOVA showed that the cutting pace is the most important element in the reactions. Furthermore, the feed cost includes the secondary charge for flank wear. The quadratic model constructed using RSM is fairly reliable and can be used to forecast the factors under study.

REFERENCES

1. Pariona, M. M., Taques, A. F., & Woiciechowski, L. A. (2018). The Marangoni effect on microstructure properties and morphology of laser-treated Al-Fe alloy with single track by FEM: Varying the laser beam velocity. *International Journal of Heat and Mass Transfer*, 119, pp. 10-19.
2. Tianchi, Y., Yuxiang, C., Xin, Y., Zhijun, L., & Jiacheng, J. (2018). Parameters of Laser Cutting Ni-Based Alloy Steel with Factors Interaction. *Laser & Optoelectronics Progress*, 2, pp. 45.
3. Peirovi, S., Pourasghar, M., Nejad, A. F., & Hassan, M. A. (2017). A study on the different finite element approaches for laser cutting of aluminum alloy sheet. *The International Journal of Advanced Manufacturing Technology*, 93(14), pp. 1399-1413.
4. Venkatesan, K., Kanubhai, J., Raval, G. V., & Vipulkumar, S. H. (2018). A Study On Prediction Of Forces And Cutting Temperature In Laser-Assisted Machining Of Inconel 718 Alloy Using Numerical Approach. *Materials Today: Proceedings*, 5(5), pp. 12339-12348.
5. Lamikiz, a., Lacalle, L. N. L. De, Sánchez, J. a., Pozo, D. Del, Etayo, J. M., & López, J. M. (2015). CO2 laser cutting of advanced high strength steels (AHSS). *Applied Surface Science*, 242, pp. 362-368. <http://doi.org/10.1016/j.apsusc.2004.08.039>

6. Yilbas, B. S. (1998). Study of Parameters for CO₂ Laser Cutting Process. *Materials & Manufacturing Processes*, 13, pp. 517-536.
7. Pfeifer, Herzog, Hustedt, & Barcikowski, 2010. Pulsed Nd : YAG laser cutting of NiTi shape memory alloys Influence of process parameters. *Journal of Materials Processing Tech.*, 210(14), pp. 1918-1925. <http://doi.org/10.1016/j.jmatprotec.2010.07.004>
8. Baghjari, S. H., & AkbariMousavi, S. A. A. (2014). Experimental investigation on dissimilar pulsed Nd: YAG laser welding of AISI 420 stainless steel to kovar alloy. *Materials & Design*, 57, pp. 128-134.
9. Baghjari, S. H., & Mousavi, S. A. A. A. (2013). Effects of pulsed Nd: YAG laser welding parameters and subsequent post-weld heat treatment on microstructure and hardness of AISI 420 stainless steel. *Materials & Design*, 43, pp. 1-9
10. Da Sun, S., Fabijanic, D., Barr, C., Liu (2018). In-situ quench and tempering for microstructure control and enhanced mechanical properties of laser clad AISI 420 stainless steel powder on 300M steel substrates. *Surface and Coatings Technology*, 333, pp. 210-219.
11. Yilbas, B. S., Khan, S., Raza, K., & Keles, O. (2010). Laser cutting of 7050 Al alloy reinforced with Al₂O₃ and B₄C composites, pp. 185-193. <http://doi.org/10.1007/s00170-009-2489-6>
12. Ahn, D. G., Byun, K. W., & Kang, M. C. (2010). Thermal Characteristics in the Cutting of Inconel 718 Superalloy using CW Nd: YAG Laser. *Journal of Materials Science and Technology*, 26(4), pp. 362-366. [http://doi.org/10.1016/S1005-0302\(10\)60059-X](http://doi.org/10.1016/S1005-0302(10)60059-X)
13. Cekic, A., Begic-Hajdarevic, D., Kulenovic, M., & Omerspahic, A. (2014). CO₂ laser cutting of alloy steels using N₂ assist gas. *Procedia Engineering*, 69, pp. 310-315.
14. Leone, C., Genna, S., Caggiano, A., Tagliaferri, V., & Moliterno, R. (2015). An investigation on Nd: YAG laser cutting of Al 6061 T6 alloy sheet. *Procedia CIRP*, 28, pp. 64-69.
15. Yan, Y., Li, L., Sezer, K., Whitehead, D., Ji, L., Bao, Y., & Jiang, Y. (2012). Nano-second pulsed DPSS ND: YAG Laser striation-free cutting of alumina sheets. *International Journal of Machine Tools and Manufacture*, 53(1), pp. 15-26. <http://doi.org/10.1016/j.ijmachtools.2011.07.006>
16. Akbari, M., Saedodin, S., Toghraie, D., Shoja-Razavi, R., & Kowsari, F. (2014). Experimental and numerical investigation of temperature distribution and melt pool geometry during pulsed laser welding of Ti6Al4V alloy. *Optics & Laser Technology*, 59, pp. 52-59.
17. Antar, M., Chantzis, D., Marimuthu, S., & Hayward, P. (2016). High speed EDM and laser drilling of aerospace alloys. *Procedia Cirp*, 42, pp. 526-531.
18. Cekic, A., Begic-Hajdarevic, D., Kulenovic, M., & Omerspahic, A. (2014). CO₂ laser cutting of alloy steels using N₂ assist gas. *Procedia Engineering*, 69, pp. 310-315
19. Adelman, B., & Hellmann, R. (2011). Fast Laser Cutting Optimization Algorithm. *Physics Procedia*, 12, pp. 591-598. <http://doi.org/10.1016/j.phpro.2011.03.075>

20. Bandyopadhyay, S., Sundar, J. K. S., Sundararajan, G., & Joshi, S. V. (2002). Geometrical features and metallurgical characteristics of Nd: YAG laser drilled holes in thick IN718 and Ti 6Al 4V sheets. *Journal of Materials Processing Technology*, 127(1), pp. 83-95.
 21. Riveiro, A., Quintero, F., Lusquiños, F., Comesaña, R., & Pou, J. (2010). Parametric investigation of CO₂ laser cutting of 2024-T3 alloy. *Journal of Materials Processing Technology*, 210(9), pp. 1138-1152.
 22. Sharma et al. (Sharma et. al., 2010) applied Taguchi methodology (TM) for the experimental investigation of nickel-based superalloys sheet during the laser cutting of straight and curved profiles.
 23. Sharma, A., Yadava, V., & Rao, R. (2010). Optimization of kerf quality characteristics during Nd: YAG laser cutting of nickel based superalloy sheet for straight and curved cut profiles. *Optics and Lasers in Engineering*, 48, pp. 915-925. <http://doi.org/10.1016/j.optlaseng.2010.03.005>
-

Corresponding Author

Faisal Shameem*

Assistant Professor, Department of Mechanical & Chemical Engineering, Galgotias University, Greater Noida, Uttar Pradesh, India